ELECTRON BEAM SURFACE MODIFICATION OF Ti5Al4V ALLOY FOR BIOMEDICAL APPLICATIONS

NIKOLOVA Maria P.[1], YANKOV Emil[1], PETROV Petar[2], VALKOV Stefan[2], ORMANOVA Maria[2], ZAHARIEVA Vanya[1], TONEV Danko[1], ANDREEVA Andreana[3]

[1]University of Ruse "A. Kanchev", Faculty of Mechanical and Manufacturing Engineering, Ruse, Bulgaria, EU, mpnikolova@uni-ruse.bg
[2]Bulgarian Academy of Sciences, Institute of Electronics, Sofia, Bulgaria, EU
[3]Sofia University "St. Kliment Ohridski", Faculty of Physics, Sofia, Bulgaria, EU

Abstract

Obtaining of an appropriate implant material requires a detailed analysis of the effect of the applied surface treatments. In the particular study, the Ti5Al4V alloy was vacuum heat treated and electron beam surface modified (EBSM) by scanning electron beam and its surface characteristics were revealed by modern topographic and metallographic analysis. The studies provided an essential insight into the change of the surface characteristics - topography and surface roughness, as well as the transformations of the structure caused by the vacuum heat treatment (solution treatment and precipitation) and the subsequent EBSM. The results from the SEM, AFM, and profilometry analyses after the EBSM of the as-received, quenched and precipitated Ti5Al4V alloy were compared. The obtained results are indicative of the alloy ability to modify the desired structure, appropriate for biomedical applications.

Keywords: Titanium alloy, SEM, AFM, EBSM, surface roughness

1. INTRODUCTION

The main concern on recent developments of hard implant materials is considered to be the different modifications and treatments that usually change the mechanical strength, surface energy or its composition. It is well known that the osseointegration and micro-mechanical interlocking between bone - implant and tissue ingrowth are very much influenced by the surface morphology of Ti-based materials [1, 2]. Simultaneously, the treatment for producing the surface roughness should maintain or even increase the mechanical strength of the surface, because the fatigue limit for the Ti alloys is greatly influenced by both microstructure and surface conditions. Some roughening treatments like SLA (sandblasting and acid etching) procedure have a proven negative effect on the fatigue behavior of the material, leading to a higher susceptibility to crack initiation [3]. The electron beam surface modification (EBSM) gives the opportunity to obtain reproducible isotropic textures with regular surface pattern without any surface contamination. The process is fast and precisely controlled. It is able not only to change the surface roughness and texture but to influence the distribution of the chemical elements and the material properties. The optimal implant surfaces show wave-like structures [4] but the best bio-topography for hard implant materials is still unknown. The purpose of this study is to evaluate the surface texturing pattern and microstructure of as-received, solution treated and water quenched as well as quenched and precipitated Ti5Al4V samples with well-controlled wave-like structures generated by the scanning electron beam.

2. MATERIALS AND EXPERIMENTAL PROCEDURES

Samples with dimensions 14×14×4 mm were cut out of 16 mm thick sheet material using the electroerosion cutting method. The chemical composition of the alloy given in **Table 1**, was measured by JEOL JXCA-733

Microprobe scanning electron microscope (SEM) coupled to a WDX detector. The focused electron beam with 50 μm diameter was operated at 19.9 kV for the acquisition of the chemical composition.

Table 1 Chemical composition of the Ti5Al4V alloy (wt.%)

Chemical element	Al	V	Fe	Mn	Co	Cr	Mo	Pd	Nb	Hf	Ti
Ti5Al4V	5.2	4.4	0.14	0.11	0.065	0.002	0.17	0.15	0.36	0.036	Bal.

The as-received samples were single solution treated (ST) for 30 min at 920 °C and water quenched. Half of the specimens were precipitated (P) for 4 hours at 500 °C and air cooled. All treatments were carried out in≤1 Pa vacuum. The surfaces of the samples were grounded and polished before the EBSM. To study the effect of the surface treatment, the EBSM was applied to as-received, ST and ST and precipitated (ST+P) samples.

The electron beam surface modification (EBSM) was carried out by electron beam installation Leybold Heraeus (EWS 300/15-60). The following technological parameters were applied: electron beam current I = 20 mA, accelerated voltage U = 52 kV, speed of the samples motion v = 0.5 cm/s, electron beam frequency f = 1 kHz, electron beam diameter d = 0.5 mm and linear manner of scanning.

Two roughness measurement instruments were used: Atomic Force Microscope (AFM) and a stylus profilometer. The samples were evaluated quantitatively with respect to R_a (average roughness) and R_z (maximum roughness height) after ten times scanning with a cut-off value of 0.8 mm in a direction perpendicular to grooves caused by the local melting using a contact profilometer (Mitutoyo SJ 201 P). The AFM (Anfatec Instruments AG, Germany) was used to characterize the nano-surface topography. The curvature radius of the silicon tip was 10 nm. The measurements were realized in the non-contact mode when the tip was scanning over the studied surface at a distance of few nanometers. The 3D-images of the scanned samples were created with ANFATEC PRESENT software. Each surface was scanned five times at different locations at scanning area 30×30 μm. The data were analyzed and the average roughness parameter S_a was calculated.

The light optical microscopy was performed on the top surface and cross-section of the samples using a Nikon microscope. The 14-megapixel digital camera was adapted to the microscope and used for the image acquisition after Kroll's reagent etching. Some of the micrographs were processed by Mountains Map premium v.7 software for grain size assessment. The surface morphology and chemistry of the samples was investigated using scanning electron microscope (SEM - LYRA I XMU, Tescan) equipped with energy dispersive spectroscopy (EDX - Quantax 200, Bruker) under an accelerating beam voltage of 20 kV.

3. RESULTS AND DISCUSSIONS

Table 2 summarizes the roughness parameters identified by the profiler and AFM surface measurement for the polished and EBSM samples.

Table 2 Roughness parameters estimated by the profiler measurement and AFM surface analysis of the polished and EBSM samples.

	Roughness average R_a (μm)	Peak-to-valley roughness R_z (μm)	Mean roughness S_a (nm)	Max peak heights S_p (nm)
Polished (control)	0.12 ± 0.02	0.81 ± 0.16	-	-
As-received + EBSM	0.24 ± 0.05	1.70 ± 0.27	36.88 ± 0.07	351.7
ST + EBSM	0.22 ± 0.08	1.66 ± 0.58	46.68 ± 0.09	373.8
ST + P + EBSM	0.24 ± 0.04	1.51 ± 0.24	53.75 ± 0.1	438.8

All treated samples exhibited micro-roughened topography (**Table 2**). The surface modification resulted in the formation of wave-like surface morphology (**Figure 1**). A regular morphology of ordered patterning dominated by relatively smooth elevations and recesses was obtained. The average wave-to-wave distance for the titanium surfaces was approximately 174 - 240 μm (**Figure 1**) for the three EBSM samples. The R_a average values were equal to 0.22 - 0.24 μm while the R_z values ranged from 1.51 to 1.70 μm. From the differences in the roughness values as determined by the profiler it was clear, that the surface response and the obtained morphology after the EBSM were sensitive to the initial heat treatment of the substrate. Quantitatively, the larger surface area and spaces between the peaks could act like biologically active scaffold providing more surface area for bone interlocking. It was shown that EBSM samples with a surface roughness of fewer than 0.5 μm produced the ideal biocompatibility, in comparison to solid Ti6Al4V [5].

AFM was used in order to understand the small-size roughness pattern generated within the wave-like structures. The AFM probing of 30×30 μm sampling area of the field located on the top furrow revealed that the average roughness S_a ranged between 37 and 54 nm while the S_p parameters reached values of 352 - 439 nm (**Table 2**). This non-uniform small size patterning was a result of the diffusionless β → α' - martensite transformation occurring within the surface re-melted zone during the electron-beam scanning. The precipitated martensite laths with a size of several micrometers followed a strong angular preferential orientation (**Figure 1 a, b** and **c**). In the case of the as-received EBSM sample (**Figure 1a**) the edges of the grain boundaries looked sharper than those of the ST (**Figure 1b**) and ST+P (**Figure 1c**) specimens where the grains appeared to have more rounded shape. Although the identified differences, the S_a and S_p values for all samples were in the same order of magnitude.

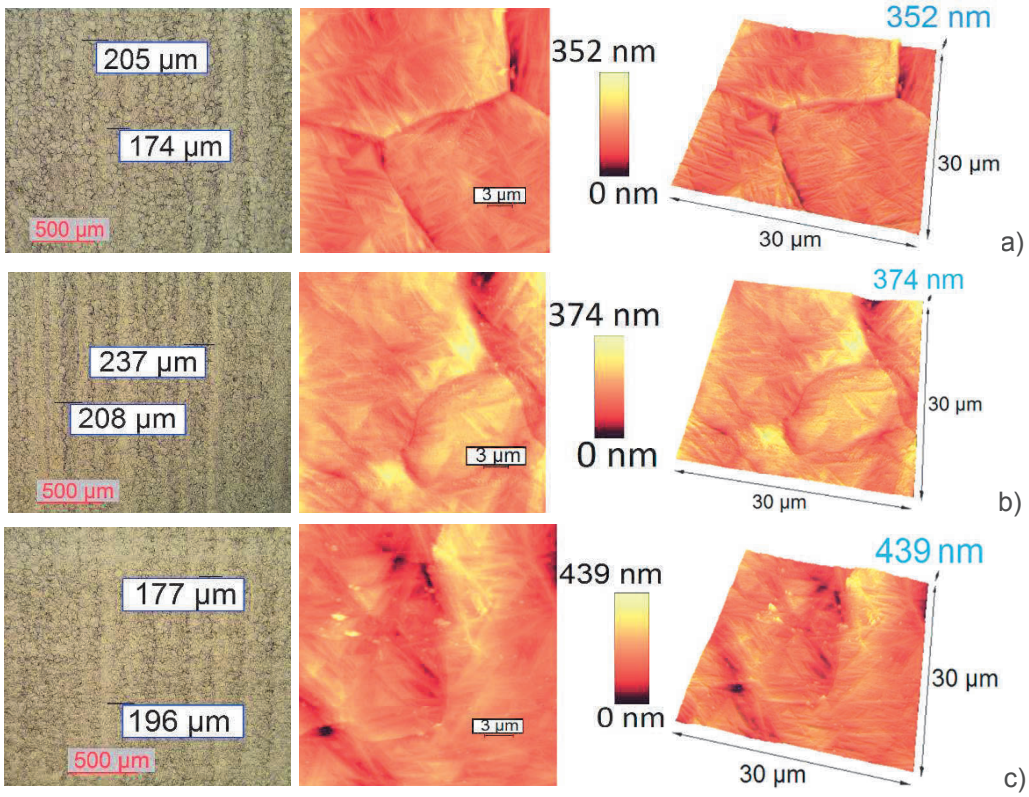

Figure 1 Top surface optical micrographs and AFM 2D and 3D images of the EBSM titanium alloy: a) as-received + EBSM; b) ST + EBSM; c) ST + P + EBSM

The re-solidified layer formed by the electron-beam irradiation was differently structured within the non- and heat treated substrate materials (**Figure 2**). The shape and size of the initial grains were changed to equiaxed

smaller grains because of the high cooling rates. As a result of the electron beam irradiation parameters, the heat conduction effect on the surface was small and the melting occurred only near to the surface. Nevertheless, the heat affected zone determined by the cross-section microstructure reached values of 263, 328 and 341 μm for the as-received, ST and ST+P samples, respectively. This difference in depth could be attributed to the thermodynamic stability of the alloy in different heat treated conditions. For the as-received sample, the smaller depth of the electron-beam affected zone suggested that the beam energy was concentrated closer to the surface thus leading to increase in the re-melted grain size.

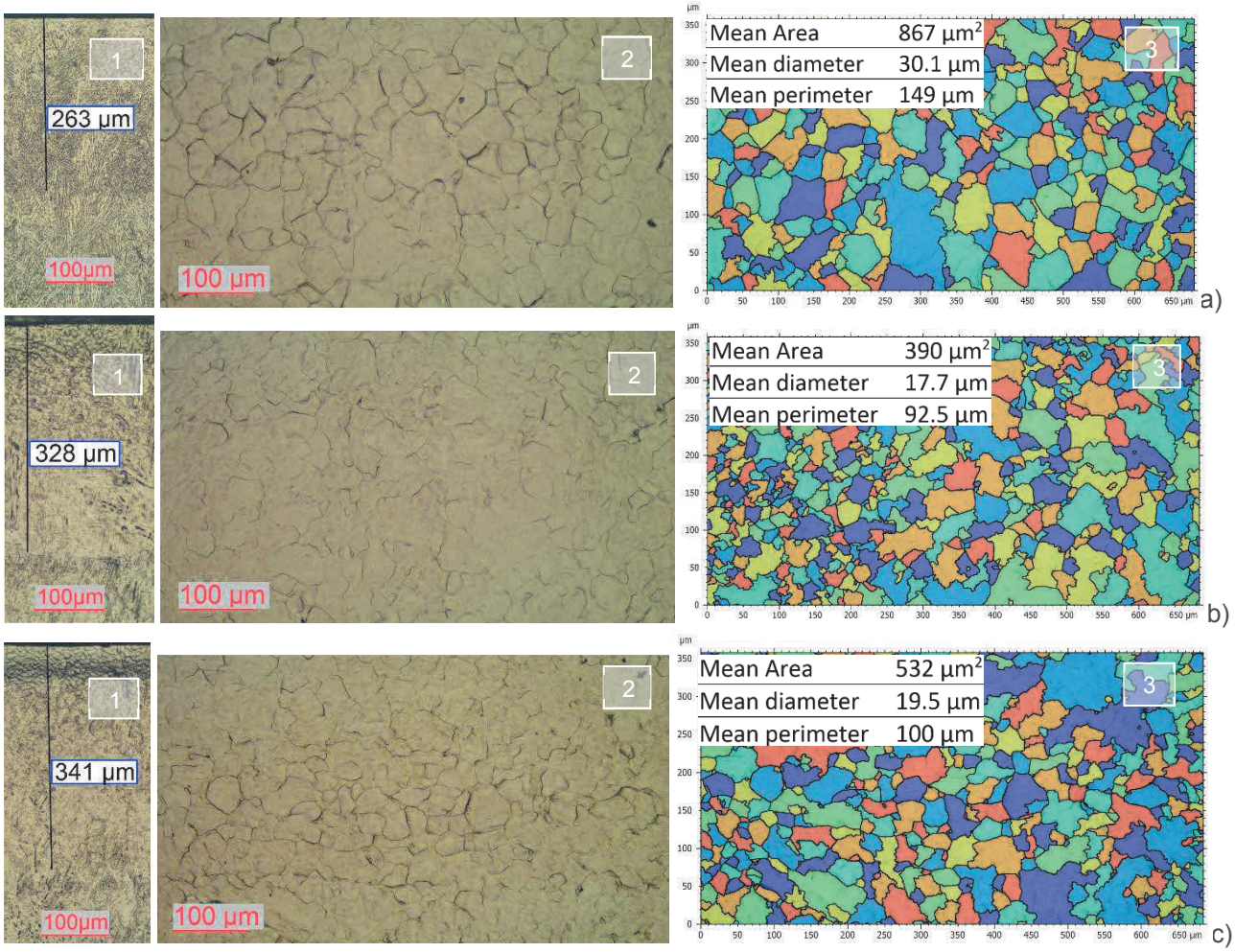

Figure 2 Optical micrographs of the EBSM samples: a) the as-received; b) ST and c) ST+P. The numbering indicates: 1) cross-section micrographs; 2) top view; 3) software processed top view image

In order to determine the surface grain size in details, a software analysis of the optical micrographs was carried out (**Figures 2a-3, 2b-3** and **2c-3**). In general, the size of the crystal grains near to the surface of all EBSM samples was smaller than that located far from the surface (**Figures 2a, b,** and **c-1**). In contrast to the as-received+EBSM sample where the average grains' area reached 867 μm^2 (**Figure 2a-3**), the mean area of the grains of the ST+EBSM and ST+P+EBSM specimens (**Figure 2b** and **c-3**) reduced to 390 and 532 μm^2, respectively, whereas the mean diameter decreased from 30 μm for the as-received to 17.7 and 19.5 μm for the ST+EBSM and ST+P+EBSM specimens, respectively. The smaller grain size obtained on the surface of the ST sample (**Figure 2b-2** and **3**) suggested more even heat distribution in depth of this specimen. This was also confirmed by the smooth, gradual change in cross-section microstructure (**Figure 2b-1**). In contrast, the precipitated alloy (**Figure 2c-3**) tended to form coarser re-melted grains than the ST+EBSM sample. As seen

from the cross-section of the ST+P+EBSM sample (**Figure 2c-1**) the change in the structure was non-homogeneous in depth and a thicker near-surface area was formed. Therefore, the pre-disposed to transformation tense microstructure of the ST+P sample distributed the beam energy unevenly in depth. The intense formation of coarser semi-coherent and non-coherent precipitates in this near-surface area could explain this phenomenon. It is worth saying that as the treatment affects the bulk structure and properties of the alloy, it would be essential for maintaining high surface hardness, toughness, and corrosion resistance.

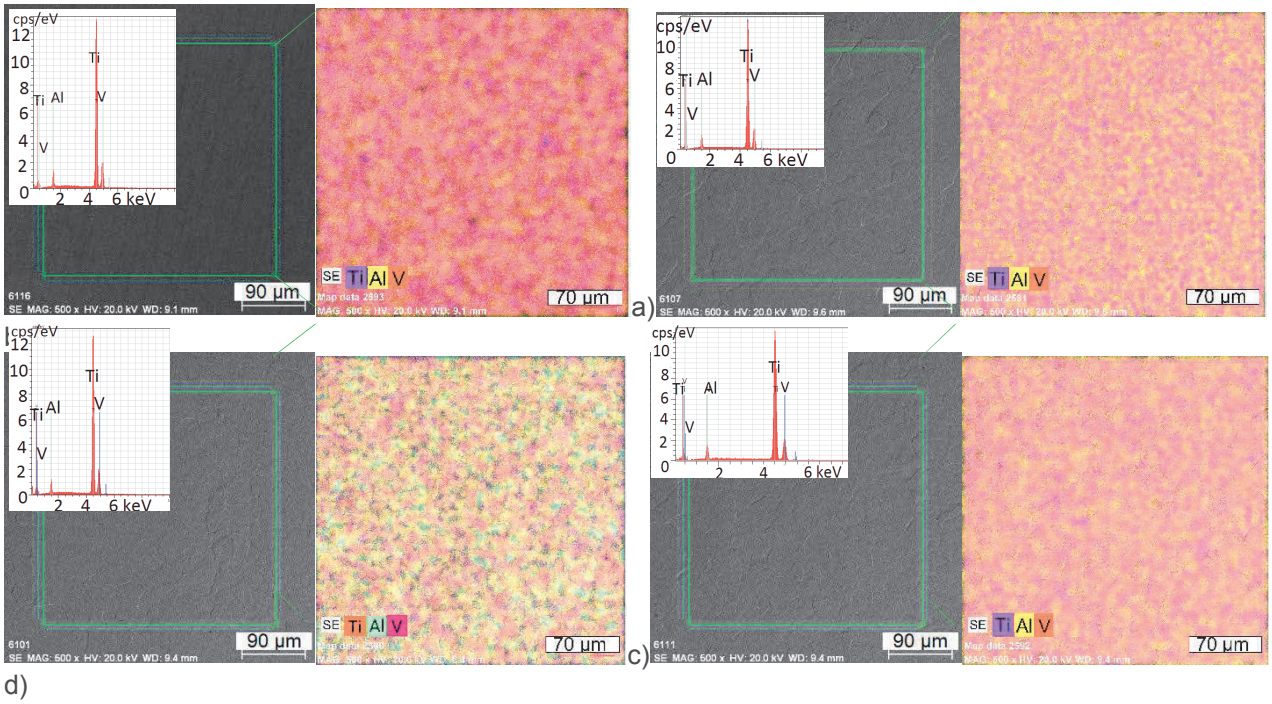

Figure 3 SEM images with their corresponding EDX pattern and element mapping: a) as-received (control) material; b) as-received+EBSM alloy; c) ST+EBSM sample; d) ST+P+EBSM sample

Figure 3 shows the SEM images of the surface morphologies with the corresponding spectrum of the chemical elements of the control sample and the EBSM ones. The control surface (**Figure 3a**) was relatively smooth and free of scratches with no significant microstructural features. The determined chemical composition confirmed that the surface layer before and after the modification consisted of similar quantities of Ti, Al, and V and no contamination occurred during the surface treatment (**Figure 3 b, c** and **d**) as the specimens showed a low concentration of contaminants like C, N, etc. The energy distribution type X-ray spectrum indicated that there was a difference in the elements' distribution while the chemical composition of the surface (**Figure 3**) was not changed by the EBSM. The spatial distribution of Ti, Al, and V after the EBSM treatment confirmed and corresponded to the micrograph observations and statistical surveys of the surface morphologies. In contrast to the non-homogenous element distribution in the control material, the surface of the EBSM specimens indicated more uniform and refined element map. Despite the relative coarser grain size, the as-received+EBSM sample (**Figure 3b**) displayed finely dispersed elements in them. Similar fine distribution of the elements was seen for the smaller sized grains of the ST+EBSM alloy (**Figure 3c**). In the case of the ST+P+EBSM (**Figure 3d**) the areas with predominant Ti and Al-content increased in size that proved the occurring phase separation during the surface treatment. As seen from the element mapping of all EBSM specimens, the Ti, Al, and V distribution was more homogenous without regard to the direction perpendicular and parallel to the grooves caused by the local melting. The low amount of detected oxygen near to the surface suggested that the high kinetic energy of the beam did not introduce contaminants in the alloy for the short term heating of the material. Some oxides settled on the peaks could form the nano-sized particles visible at

AFM pictures (**Figure 1**) because of a selective oxidation of the finely distributed elements at the surface of the alloy.

4. CONCLUSION

In this study, the structure and some surface characteristics of the EBSM Ti5Al4V alloy before and after heat treatment were investigated. The successfully obtained surface structuring with a wave-like morphology showed micro-patterning as a result of the direct beam modification. The main outcomes from the applied surface modification treatment are a higher degree of spatial organization, highly efficient isotropic micro-roughening with regular morphology, martensite transformation within the surface re-melted area, grain refinement and changes in the elements distribution (homogenization).

The established surface modification would inevitably influence the phase composition, mechanical and electrochemical properties of the each treated sample and all of these changes should be identified. The optimal surface parameters and properties of the implant material should be determined depending on the conditions of hard implant operation (corrosive environment, loading, stress shield, bone properties, etc.).

ACKNOWLEDGEMENTS

The financial support of this work was provided by the National Science Fund of Ministry of Education and Science, Bulgaria, under Grant project "Gradient functional nanocoatings produced by vacuum technologies for biomedical applications" with number DN№ 07/3 (2016).

REFERENCES

[1] SHUILIN WU, XIANGMEI LIU, KELVIN W.K. YEUNG, HUAN GUO, PENGHUI LI, TAO HU, C.Y. CHUNG, PAUL K. CHU Surface nano-architectures and their effects on the mechanical properties and corrosion behavior of Ti-based orthopedic implants. *Surface & Coatings Technology*, 2013, vol. 233, pp 13-26.

[2] WEN-CHENG CHEN, YA-SHUN CHEN, CHIA-LING KO, YI LIN, TZU-HUANG KUO, HSIEN-NAN KUO Interaction of progenitor bone cells with different surface modifications of titanium implant. *Materials Science and Engineering C*, 2014, vol. 37, pp 305-313.

[3] MEDVEDEV, A. E., MOLOTNIKOV, A., LAPOVOK, R. et al. Microstructure and mechanical properties of Ti - 15Zr alloy used as dental implant material. *J. Mech. Behav. Biomed. Mater*, 2016, vol. 62, pp 384-398.

[4] CELEN, S., ÖZDEN, H. Laser-induced novel patterns: As smart strain actuators for new-age dental implant surfaces. *Applied Surface Science*, 2012, vol. 263, pp 579-585.

[5] SHAHALI, H., JAGGESSARA, A., YARLAGADDA, P. KDV Recent advances in manufacturing and surface modification of titanium orthopaedic applications. *Procedia Engineering*, 2017, vol. 174, pp 1067- 1076.